Primary User Localization in Cognitive Radio Networks

A Dissertation

Submitted in partial fulfillment of

the requirements for the award of the degree

of

Master of Technology

in

ELECTRONICS AND COMMUNICATION ENGINEERING

with Specialization in Communication Systems

By

Abhinav

(Enrollment No. 17531002)

DEPTT. OF ELECTRONICS AND COMMUNICATION ENGINEERING

INDIAN INSTITUTE OF TECHNOLOGY,ROORKEE

ROORKEE-247667(INDIA)

MAY 2019

CANDIDATE'S DECLARATION

I declare that the work presented in this dissertation with title "**Primary User Localization in Cognitive Radio Networks**" towards the fulfillment of the requirement for the award of the degree of **Master of Technology** submitted in the **Department of Electronics and Communication Engineering**, **Indian Institute of Technology Roorkee**, India is an authentic record of my own work carried out under the supervision of **Dr. Anshul Tyagi**, Assistant Professor, Department of Electronics and Communication Engineering, IIT Roorkee.

The content of this dissertation has not been submitted by me for the award of any other degree of this or any other institute.

DATE : ..... SIGNATURE:

PLACE: ..... (Abhinav)

CERTIFICATE

This is to certify that the statement made by the candidate is correct to the best of my knowledge and belief.

DATE : ..... SIGNATURE:

(Dr. Anshul Tyagi)

Assistant Professor

Dept. of ECE

IIT Roorkee

ACKNOWLEDGEMENT

I take this opportunity to express my profound gratitude to **Dr. Anshul Tyagi** (Asst. Prof., ECE Dept., IIT Roorkee) whose exemplary guidance and continued support was a source of inspiration for me throughout the course of this work. I would also like to thank almighty and my parents for their constant encouragement.

Date : .....

Place : Roorkee (Abhinav)

Abstract

Information regarding licensed primary user (PU) space positioning can allow enabling of several important attributes in cognitive radio (CR) networks such as intelligent location-aware routing, improved spatio-temporal sensing, along with aiding spectrum policy enforcement. In this work, the issue of PU location estimation in presence of CRs which are outlier is dealt with. This is an noteworthy problem to address practically as in many real-world scenarios the CRs reports unreliable information. Therefore, firstly the accuracy that PU localization algorithms can achieve by jointly utilizing direction of arrival (DoA) and received signal strength (RSS) measurements is considered by evaluation of Cramer-Rao Bound (CRB). In past research, CRB for DoA-only and RSS-only localization algorithms are evaluated separately and estimation error variance of DoA is assumed to be independent of RSS. In this work, for joint RSS and DoA-based PU localization algorithms, CRB is evaluated which is based on mathematical model in which DoA is dependent on RSS. The bound is then used in futher work to examine the performance of PU localization algorithms and impact of number of CRs is discussed. CRB for uniform random CR deployment is also derived and studies are performed to find out number of CRs tightly approximate integration of CRB for fixed CR placement by asymptotic CRB.

Following that statistics techniques are applied on squared range measurements and two different methods are implemented for solving the task of PU localization in presence of outlying CRs. The first approach is efficient in terms of computational complexity, but only objective convergence is guaranteed theoretically in that approach. Contrary to that, whole-sequence convergence is established for second method . In order to take benefits of both the approaches, a hybrid algorithm is developed by integrating both the approaches that offers computational efficiency along with whole-sequence convergence.Simulations show that robust methods meet the CRB for large number of CRs. For small number of CR measurements, the implemented robust methods does not achieve CRB but performs better than other localization methods implemented in this work.

Contents

List of Figures

Abbreviations

CR	Cognitive Radio
PU	Primary User
GPS	Global Positioning System
WSN	Wireless Sensor Network
SNR	Signal-to-Noise Ratio
ToA	Time-of-Arrival
SR	Squared-Range
DoA	Direction-of-Arrival
TW-ToF	Two-Way Time-of-Flight
RSS	Received-Signal Strength
TDoA	Time Difference-of-Arrival
LS	Least-Squares
ML	Maximum Likelihood
CRB	Cramer-Rao Bound
GTRS	Generalized Trust Region Subproblem
IRLS	Iteratively Reweighted Least Squares
ULA	Uniform Linear Array
FIM	Fisher Information Matrix
WCL	Weighted Centroid Localization
SRLS	Square-Range-Based Least Squares
GM	Geman-McClure
SR-IRLS	Squared Range Iterative Reweighted Least Square
SR-GD	Squared Range Gradient Descent
SR-LS	Square Range Least Square
SR-Hybrid	Squared Range Hybrid
RMSE	Root Mean Square Error
AWGN	Additive White Gaussian Noise
SU	Secondary User

Chapter 1

Introduction

Cognitive Radio (CR) is one of the approaches which promises to utilize the scarce RF spectrum resources in a efficient manner [2]. In this respect, information regarding spectrum occupied with respect to space, frequency, and time which is precise and timely is necessary for allowing CR for using spectrum in a opportunistic manner and for avoidance of interference to primary users (PU) [3]. Particularly, knowledge about PU position could help to enable several important attributes in CR networks including intelligent location-aware routing, improved spatio-temporal sensing, as well as aiding in enforcement of spectrum policies [4].

The task of PU localization in CR networks differs from localization in other applications such as Global Positioning System (GPS) and Wireless Sensor Networks (WSN), because of following reasons. Firstly, PU does not communicate or cooperate with CRs as they use spectrum bands of PU opportunistically. So, limited information regarding PU signalling, such as modulation scheme or transmit power, is known by CRs. Therefore, passive localization methods can be used. Secondly, as detection and localization of PUs by the CRs is required to be done at a very low SNR throughout the whole coverage area for avoiding interfering to primary user, the number of CRs needed is large and it is necessary for CRs to cooperate among themselves.

1.1 Background and Literature Survey

The localization problem occurs in various areas such as navigation surveillance, and acoustics. There are various methods for localizing based on different types of measurements such as time-of-arrival (ToA), squared-range (SR), direction-of-arrival (DoA), two-way time-of-flight (TW-ToF), and received-signal strength (RSS).

Past researches can be classified to different categories depending upon type of measurement exchanged among CRs to get the estimate of the location [5]. RSS based algorithms made use of received power measured from PU to provide location estimates at low computational and hardware complexity. TDoA based algorithms give location estimate using differences of time among multiple reception of signal that is transmitted. They are unsuitable for localization in CR networks as perfect synchronization among CRs is required in TDoA-based algorithms. DoA based algorithms make usage of estimates of target DoA, which is observed at different receivers, in order to obtain estimates of location.

Localization using range and range difference are considered in [6]. Popular DoA fusion algorithm includes Stansfield algorithm [7] and Maximum Likelihood (ML) [8] and both of them provides different trade-off between complexity and complexity. Weighted version of DoA fusion algorithm improves the accuracy of localization [8]. The weight is generally estimated by error variance of DoA measurement, which is acquired using RSS [9]. ToA estimation error is modeled as Cauchy-Lorentz distribution in the method implemented in [10]. In [11], robust statistics is exploited by usage of position of subset of nodes for localization of sensors in a network. Authors in [12] try to get location estimates using TW-ToF by minimizing worst-case likelihood function and employing semidefinite relaxation.

In this dissertation, the task of PU localization is examined. In CR networks, there is a possibility that some CRs might report incorrect information maliciously or unintentionally. This generally occurs due to physical obstruction of the scene, low battery, network failures, and attackers. Thus, there should not be simple aggregation of measurements provided by sensor nodes by the processing node. It will be better to localize the PU based on reliable measurements and disregard the outlier measurements.

In the present work, performance of different localization algorithms is compared with respect to number of CRs and their achievable accuracy is obtained using CRB, which lower bounds estimation accuracy for an estimator which is unbiased. The CRB evaluation using RSS-only localization is well studied in [5] which makes assumption of correlated and independent shadowing channels. The DoA-only CRB is well studied in various papers [13], but all of them have assumed that estimate of DoA from CRs are subjected to independent and identically distributed gaussian errors having zero mean and fixed variance. As DoA estimation error variance is dependent on RSS and other factors (e.g. array orientation error) [9], therefore assuming it to be fixed result in inaccurate

derived bounds.

In this dissertation, the primary objective is localizing a single PU when range measurements of outlier is present cooperatively. The contributions of this dissertation are summed as follows. Firstly, CRB of joint RSS and DoA-based localization, considering interdependence of RSS and DoA, is derived. The CRB is evaluated for MUSIC algorithm and optimal DoA estimator, where the error is provided by CRB of DoA estimation error variance. Hence, derived CRB helps in providing ultimate achievable accuracy. Next, practical localization algorithm (WCL and W-Stansfield) is implemented to show how close the CRB can be achieved. Then, two different methods are implemented for finding solution of localization issue in presence of outliers. In the first algorithm, the proposed localization problem is converted to GTRS [14], based of the IRLS. Numerical simulations infers that IRLS method provides objective convergence which is fast but in this algorithm whole-sequence does not converges. The second method is globally convergent, but requires more time to converge. By combining these two method, a hybrid method is implemented having desired attributes, such as whole-sequence convergence requiring less number of iterations.

Chapter 2

Joint CRBs Derivation For Given CR Placement

2.1 System Model

N CRs are assumed to cooperate to localize single PU. 2-dimensional location of the PU and n^{th} CR is denoted as $\ell_P = [x_P, y_P]^T$ and $\ell_n = [x_n, y_n]^T$, respectively. All locations are fixed in the observation period, and CR locations are defined. RSS and DoA are available measurements at CRs. RSS measurement is modelled as $\hat{\psi}_n \triangleq P_T \frac{c_0 10^{-sn/10}}{d_n^{\gamma}}$ Watt at the n^{th} CR, where $\mathrm{P_T}$ is PU transmit power, c_0 is average multiplicative gain (constant) at reference distance, $d_n = \|\ell_n - \ell_P\|$ is the euclidean distance between the PU and n^{th} CR, γ is path loss exponent, and $10^{-s_n/10}$ is random variable that reflects shadowing. The RSS is generally expressed in dBm using the given transformation $\hat{\phi}_n = 10\log_{10}(1000\psi_n)$. The result is expressed as:

$$\hat{\phi}_n = 10\log_{10}(1000 P_T c_0) - 10\gamma \log_{10} d_n - s_n \triangleq \overline{\phi}_n - s_n \tag{2.1}$$

The collection of RSS measurements of all CRs is denoted as $\hat{\boldsymbol{\phi}} = \left[\hat{\phi}_1, \hat{\phi}_2, \ldots, \hat{\phi}_N\right]^T$. The conditional distribution of $\hat{\phi}$ (for given ℓ_P) is $\hat{\phi} \sim \mathcal{N}\left(\overline{\phi}, \Omega_s\right)$, where $\overline{\phi} = \left[\overline{\phi}_1, \overline{\phi}_2, \ldots, \overline{\phi}_N\right]^T$ and Ω_s is covariance matrix of the collections of shadowing variables $\mathbf{s} = [s_1, s_2, \ldots, s_N]^T$, given by $\{\Omega_s\}_{mn} = \sigma_s^2 e^{-\|\ell_m - \ell_n\|/X_C}$, where X_c denotes correlation distance within which there is correlation of shadowing effects among nodes. The DoA of PU at n^{th} CR is expressed as $\theta_n \triangleq \arctan\left(\frac{y_P - y_n}{x_P - x_n}\right) \triangleq \angle(\ell_P, \ell_n)$. CRs perform signal processing techniques on arrays, such as MUSIC [19], to obtain DoA estimate. The estimated DoA is generally modelled as $\widehat{\theta}_n \triangleq \theta_n + v_n$, where $v_n \sim \mathcal{N}(0, \sigma_n^2)$ and σ_n^2 is DoA estimation error variance. The collections of DoA measurements of all CRs at the fusion

centre is denoted as $\widehat{\boldsymbol{\theta}} = \left[\widehat{\theta}_1, \widehat{\theta}_2, \ldots, \widehat{\theta}_N\right]$. Two different modelings of the DoA estimation error variance is considered, using MUSIC algorithm and CRB. The CRB of the DoA estimation error variance for the unbiased DoA estimators using an arbitrary array response is presented in [8, Sec. IV, Eqn. 4.1], the resultant for the ULA is given by [16, Sec. III-B, Eqn.20].

$$\sigma^2_{n,CRB} = \frac{1}{\left(\kappa \cos \widetilde{\theta}_n\right)^2} \frac{6}{N_s N_a \left(N_a^2 - 1\right) \rho_n} \tag{2.2}$$

where κ is a constant which is determined by signal wavelength and array spacing, N_a is number of antennas, N_s is number of samples, θ_n is array orientation with respect to incoming DoA expressed as $\tilde{\theta}_n \triangleq \theta_n - \overline{\theta}_n$, where $\tilde{\theta}_n$ is orientation of n^{th} ULA, and ρ_n is SNR given by $\rho_n = \widehat{\psi}_n / P_M$, where P_M is measurement noise power. Using definition of SNR, (2.2) can be represented as:

$$\begin{aligned} \sigma^2_{n,CRB} &= \frac{6P_M}{\kappa^2 N_s N_a \left(N_a^2 - 1\right)} \frac{1}{\widehat{\psi}_n} \frac{1}{\cos^2 \widetilde{\theta}_n} \\ &= \beta f_{CRB}\left(\widehat{\phi}_n\right) \frac{1}{\cos^2 \widetilde{\theta}_n} \end{aligned} \tag{2.3}$$

where $f_{CRB}\left(\widehat{\phi}_n\right) \triangleq \frac{1}{\widehat{\psi}_n}$ and $\beta \triangleq \frac{6P_M}{\kappa^2 N_s N_a (N_a^2 - 1)}$. The DoA estimate obtained from MUSIC are, unbiased, asymptotically in sample size and Gaussian distributed with error variance provided by [8, Sec. III-B, Eqn. 3.11]. The estimation error variance making use of ULA is expressed as [16, Sec. III-B, Eqn. 21]:

$$\begin{aligned} \sigma^2_{n,MU} &= \frac{1}{\left(\kappa \cos \widetilde{\theta}_n\right)^2} \frac{6}{N_s N_a \left(N_a^2 - 1\right) \rho_n} \left(1 + \frac{1}{N_a \rho_n}\right) \\ &= \beta f_{MU}\left(\widehat{\phi}_n\right) \frac{1}{\cos^2 \widetilde{\theta}_n} \end{aligned} \tag{2.4}$$

where $f_{MU}\left(\hat{\phi}_n\right) \triangleq \frac{\widehat{\psi}_n + (P_M/N_a)}{\widehat{\psi}_n^2}$. In PU localization problem, RSS and DoA measurements are used to obtain PU location estimate $\widehat{\ell}_P \triangleq [\widehat{x}_p, \widehat{y}_p]^T$. The RMSE of the location estimate is given by $RMSE \triangleq \sqrt{\mathbb{E}\left[\left\|\widehat{\ell}_P - \ell_P\right\|^2\right]}$. It is assumed that narrow-band signals from far field transmitters are propagated via single-path channel, thus DoA measurement and fusion are practical and possible.

2.2 Joint CRB Derivation For Fixed CR Deployment

In this module, joint CRB and corresponding bound on RMSE for fixed CR placement is derived, where DoA estimates are derived from both optimal estimator and MUSIC

algorithm. CRB and RMSE for RSS-only localization is derived as by-product. The covariance matrix of unbiased estimation of PU locations $\widehat{\ell}_P$, obtained using RSS and DoA as measurements, is lower-bounded by the CRB:

$$\Omega_{\widehat{\ell}_P} \triangleq \mathbb{E}\left[\left(\widehat{\ell}_P - \mathbb{E}\left[\widehat{\ell}_P\right]\right)\left(\widehat{\ell}_P - \mathbb{E}\left[\hat{\ell}_P\right]\right)^T\right] \geq \mathbf{F}^{-1} \tag{2.5}$$

where $\mathbf{F}$ is 2×2 Fisher Information Matrix (FIM) given by:

$$\mathbf{F} = -\mathbb{E}_{\widehat{\boldsymbol{\theta}},\widehat{\boldsymbol{\phi}}}\left[\frac{\partial^2}{\partial \ell_P^2} \log p\left(\widehat{\boldsymbol{\theta}}, \widehat{\boldsymbol{\phi}}|\ell_P\right)\right] \tag{2.6}$$

Therefore, RMSE is bounded by $RMSE \geq \sqrt{\{\mathbf{F}^{-1}\}_{11} + \{\mathbf{F}^{-1}\}_{22}}$ where ij^{th} element of matrix X is denoted by $\{\mathbf{X}\}_{ij}$. The standard decomposition of conditional probability $p\left(\widehat{\boldsymbol{\theta}}, \widehat{\boldsymbol{\phi}}|\ell_P\right) = p\left(\widehat{\boldsymbol{\theta}}|\widehat{\boldsymbol{\phi}}, \ell_P\right) p\left(\widehat{\boldsymbol{\phi}}|\ell_P\right)$is used to decompose FIM as:

$$\begin{aligned}\mathbf{F} = &\left\{-\mathbb{E}_{\widehat{\boldsymbol{\theta}},\widehat{\phi}}\left[\frac{\partial^2}{\partial \ell_P^2} \log p\left(\widehat{\boldsymbol{\theta}}|\widehat{\boldsymbol{\phi}}, \ell_P\right)\right]\right\} \\ &+ \left\{-\left\{-\mathbb{E}_{\widehat{\boldsymbol{\phi}}}\left[\frac{\partial^2}{\partial \ell_P^2} \log p\left(\widehat{\boldsymbol{\phi}}|\ell_P\right)\right]\right\} \triangleq \mathbf{F}_{\widehat{\boldsymbol{\theta}}|\widehat{\phi}} + \mathbf{F}_{\widehat{\boldsymbol{\phi}}}\right.\end{aligned} \tag{2.7}$$

It should be noted that $F_{\hat{\phi}}$ is FIM for using only RSS for localization of PU and therefore localization accuracy of algorithm that use only RSS readings is bounded by its inverse. In rest of the work, RSS-only FIM $F_{\hat{\phi}}$ is derived first and then the results for joint FIM F is obtained by derivation of $\mathbf{F}_{\widehat{\boldsymbol{\theta}}|\widehat{\phi}}$ for optimal DoA estimator and MUSIC algorithm.

2.2.1 RSS-only CRB

For derivation of RSS-only FIM $F_{\hat{\phi}}$ the logarithm of PDF of $\widehat{\phi}$ is expressed as:

$$\begin{aligned}\log p\left(\widehat{\phi}|\ell_P\right) = &-\log\left[(2\pi)^{N/2}\left(\det \Omega_{\mathrm{s}}\right)^{1/2}\right] \\ &-\frac{1}{2}(\widehat{\phi} - \overline{\phi})^T \Omega_{\mathrm{s}}^{-1}(\widehat{\phi} - \overline{\phi})\end{aligned} \tag{2.8}$$

The RSS-only FIM $F_{\hat{\phi}}$ is then provided by:

$$\mathbf{F}_{\widehat{\phi}} = \frac{1}{2}\mathbb{E}_{\widehat{\phi}}\left[\frac{\partial^2}{\partial \ell_P^2}(\widehat{\phi} - \overline{\phi})^T \Omega_{\mathrm{s}}^{-1}(\widehat{\phi} - \overline{\phi})\right] \tag{2.9}$$

For obtaining a compact expression, we define $\mathbf{L} = [\Delta\mathbf{x}, \Delta\mathbf{y}]^T$ and $\Lambda = \frac{1}{\epsilon\gamma^2}\mathbf{D}^2\Omega_{\mathrm{S}}\mathbf{D}^2$. Therefore, the FIM and RMSE of PU localization based on RSS-only are provided by:

$$\begin{aligned}\mathbf{F}_{\widehat{\phi}} &= \mathbf{L}\boldsymbol{\Lambda}^{-1}\mathbf{L}^T \\ \mathrm{RMSE}_{R,F} &\geq \sqrt{\left\{\mathbf{F}_{\widehat{\phi}}^{-1}\right\}_{11} + \left\{\mathbf{F}_{\widehat{\phi}}^{-1}\right\}_{22}}\end{aligned} \tag{2.10}$$

where subscript R, F denotes RSS-only bound for fixed placement.

2.2.2 Joint CRB Derivation Using Optimal DoA Estimation

In this module, joint CRB with DoA estimation is derived which is given by optimal estimator, using DoA error variance provided by $\sigma^2_{n,CRB}$. For derivation of conditional FIM of DoA given RSS $\mathbf{F}_{\widehat{\boldsymbol{\theta}}|\widehat{\boldsymbol{\phi}}}$, logarithm of conditional PDF $p\left(\widehat{\boldsymbol{\theta}}|\widehat{\boldsymbol{\phi}},\ell_P\right)$ is expressed as:

$$\begin{aligned}\log p\left(\widehat{\boldsymbol{\theta}}|\widehat{\phi},\ell_P\right) &= \log\{\prod_{n=1}^{N}\frac{1}{\sqrt{2\pi\sigma^2_{n,CRB}}}\exp\left[-\frac{\left(\widehat{\theta}_n-\theta_n\right)^2}{2\sigma^2_{n,CRB}}\right]\}\\ &=\sum_{n=1}^{N}\left\{\log\left(\cos\widetilde{\theta}_n\right)-\frac{1}{2}\log\left[2\pi\beta f_{CRB}\left(\widehat{\phi}_n\right)\right]\right.\\ &\left.-\frac{\cos^2\widetilde{\theta}_n\left(\widehat{\theta}_n-\theta_n\right)^2}{2\beta f_{CRB}\left(\hat{\phi}_n\right)}\right\}\end{aligned} \tag{2.11}$$

Therefore $\mathbf{F}_{\widehat{\boldsymbol{\theta}}|\widehat{\boldsymbol{\phi}}}$ is provided by:

$$\mathbf{F}_{\widehat{\boldsymbol{\theta}}|\widehat{\phi}}=\sum_{n=1}^{N}\left\{\mathbb{E}_{\widehat{\boldsymbol{\theta}},\widehat{\phi}}\left[\frac{\partial^2 g_n}{\partial\ell_P^2}\right]-\mathbb{E}_{\widehat{\boldsymbol{\theta}},\widehat{\boldsymbol{\phi}}}\left[\frac{\partial^2 h_n}{\partial\ell_P^2}\right]\right\} \tag{2.12}$$

where, $h_n \triangleq \log\left(\cos\widetilde{\theta}_n\right)$ and $g_n \triangleq \frac{\cos^2\widetilde{\theta}_n\left(\widehat{\theta}_n-\theta_n\right)^2}{2\beta f_{CRB}\left(\widehat{\phi}_n\right)}$. For obtaining compact expression of $\mathbf{F}_{\widehat{\boldsymbol{\theta}}|\widehat{\boldsymbol{\phi}}}$, we define $\mathbf{P}=[\Delta\mathbf{y},-\Delta\mathbf{x}]^T$ and $\Gamma=\mathrm{diag}\left(\gamma_1,\gamma_2,\ldots,\gamma_N\right)$, where $\gamma_n=\frac{1}{d_n^4}\left\{\frac{\alpha\cos^2\widetilde{\theta}_n}{d_n^\gamma}+2\tan^2\widetilde{\theta}_n\right\}$. Therefore, it can be verified that $\mathbf{F}_{J,F,C}=\mathbf{P}\Gamma\mathbf{P}^T$. So, the joint FIM and corresponding RMSE are provided by:

$$\begin{aligned}\mathbf{F}_{J,F,C}&=\mathbf{P}\Gamma\mathbf{P}^T+\mathbf{L}\Lambda^{-1}\mathbf{L}^T\\ \mathrm{RMSE}_{J,F,C}&\geq\sqrt{\left\{\mathbf{F}^{-1}_{J,F,C}\right\}_{11}+\left\{\mathbf{F}_{J,F,C}\right\}_{22}}\end{aligned} \tag{2.13}$$

where subscript J,F,C denotes joint CRB for fixed CR placement using CRB of the DoA estimation error variance.

2.2.3 Joint CRB Derivation Using MUSIC Algorithm

In this module, joint CRB with DoA estimation provided by MUSIC algorithm, using error variance provided by $\sigma^2_{n,MU}$ is derived. The conditional FIM $\mathbf{F}_{\widehat{\boldsymbol{\theta}}|\widehat{\boldsymbol{\phi}}}$ of DoA given RSS is obtained by replacement of $f_{CRB}\left(\hat{\phi}_n\right)$ in (2.11) with $f_{MU}\left(\hat{\phi}_n\right)$ given by (2.4). By application of results obtained previously, $\mathbf{F}_{\widehat{\boldsymbol{\theta}}|\widehat{\phi}}=\mathbf{P}\boldsymbol{\Delta}\mathbf{P}^T$ is obtained, where $\boldsymbol{\Delta}=\mathrm{diag}\left(\delta_1,\delta_2,\ldots,\delta_N\right)$ and

$$\begin{aligned}\delta_n=&\frac{1}{d_n^4}\left\{\frac{\cos^2\widetilde{\theta}_n}{\beta}\left[\frac{c_0P_Te^{\sigma_s^2/(2\epsilon)}}{d_n^\gamma}-\frac{P_M}{N_a}\right.\right.\\ &\left.\left.+\frac{P_M^2}{N_a^2}\mathbb{E}_{\widehat{\phi}}\left(\frac{1}{\widehat{\psi}_n+\frac{P_M}{N_a}}\right)\right]+2\tan^2\widetilde{\theta}_n\right\}\end{aligned} \tag{2.14}$$

As RSS-only FIM is not dependent on DoA estimation algorithm, the joint FIM and corresponding RMSE obtained using MUSIC algorithm are provided by:

$$\begin{aligned} \mathbf{F}_{J,F,M} &= \mathbf{P}\Delta\mathbf{P}^T + \mathbf{L}\mathbf{\Lambda}^{-1}\mathbf{L}^T \\ \text{RMSE}_{J,F,M} &\geq \sqrt{\left\{\mathbf{F}_{J,F,M}^{-1}\right\}_{11} + \left\{\mathbf{F}_{J,F,M}\right\}_{22}} \end{aligned} \tag{2.15}$$

where subscript J, F, M denotes joint CRB for fixed CR placement using error variance provided by MUSIC algorithm.

2.3 Joint CRB Derivation For Uniform Random CR Deployment

The RMSE bounds obtained in Section 2.2 are useful in evaluating the achievable localization performance for fixed CR placement. For obtaining average accuracy for random CR placement, ensemble averaging or numerical integration is required to be performed. In this module, the achievable localization accuracy for uniform random placement is discussed by deriving closed form asymptotic CRB for such case and assuming optimal DoA estimator and i.i.d. shadowing.

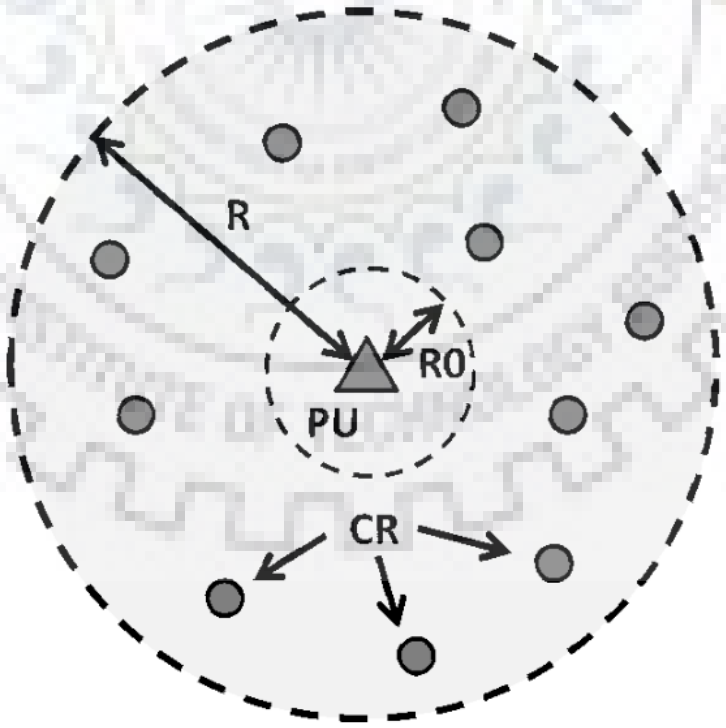

Fig. 2.1. Circular model of CR Deployment [1].

It is assumed that CRs hearing PU form a circle having radius R and are uniformly dis-

tributed in the area, as shown in Fig. 2.1. The CRs are distributed independently within the circumference of circle, which indicates all θ_n's and all d_n's are independent. Considering this scenario, distribution of θ_n is provided by $\theta_n \sim \mathcal{U}[0, 2\pi)$, and the distribution of d_n is expressed as:

$$p_{d_n}(r) = \begin{cases} \frac{2r}{\left(R^2 - R_0^2\right)}, & R_0 \leq r \leq R \\ 0, & \text{otherwise} \end{cases} \tag{2.16}$$

where R_0 denotes guard distance required for avoiding overlapping of CRs and PU.

2.3.1 RSS-only CRB For Uniform Random CR Deployment

For RSS-only FIM $\mathbf{F}_{\widehat{\phi}}$ with i.i.d. shadowing, using (2.10) it can be rewritten as:

$$\frac{1}{N}\mathbf{F}_{\widehat{\phi}} = \frac{\epsilon\gamma^2}{\sigma_s^2 N}\sum_{n=1}^{N} d_n^{-2} \begin{bmatrix} \cos\theta_n \\ \sin\theta_n \end{bmatrix} [\cos\theta_n, \sin\theta_n] \tag{2.17}$$

in which the fact is used that $[\Delta x_n, \Delta y_n] = [d_n \cos\theta_n, d_n \sin\theta_n]$. $\frac{1}{N}\mathrm{F}_{\hat{\phi}}$ is interpreted as ensemble average of function of random variables θ_n and d_n and its statistical mean is provided by:

$$\begin{aligned} \frac{1}{N}\mathbb{E}\left[\mathbf{F}_{\widehat{\phi}}\right] &= \frac{\epsilon\gamma^2}{2\sigma_s^2}\mathbb{E}_{d_n}\left[d_n^{-2}\right]\mathbf{I}_2 = \frac{\epsilon\gamma^2 \log\left(R/R_0\right)}{\sigma_s^2\left(R^2 - R_0^2\right)}\mathbf{I}_2 \\ &\triangleq f_{\widehat{\phi}}\left(R, \gamma, \sigma_s^2\right)\mathbf{I}_2 \end{aligned} \tag{2.18}$$

where first equality is obtained from (2.17) which is based on i.i.d. distribution of θ_n and d_n, and $\mathbb{E}_{\theta_n}\left\{[\cos\theta_n, \sin\theta_n]^T [\cos\theta_n, \sin\theta_n]\right\} = \frac{1}{2}\mathbf{I}_2$, where $\mathbf{I}_2$ denotes 2×2 identity matrix. The deviation probability of ensemble average $\frac{1}{N}\mathrm{F}_{\hat{\phi}}$ from statistical mean $\frac{1}{N}\mathbb{E}\left[\mathbf{F}_{\hat{\phi}}\right]$ is provided by following theorem.

Theorem 1: (Deviation Probability of RSS-only FIM) : For $\delta_0 > 0$,we have

$$\begin{aligned} &\Pr\left\{\left\|\tfrac{1}{N}\mathbf{F}_{\widehat{\phi}} - \tfrac{1}{N}\mathbb{E}\left[\mathbf{F}_{\widehat{\phi}}\right]\right\|_F > \delta_0\right\} \\ &< \tfrac{2\epsilon^2\gamma^4}{\sigma_s^4\delta_0^2 N}\left[\tfrac{1}{2R^2R_0^2} - \tfrac{\log^2(R/R_0)}{\left(R^2 - R_0^2\right)^2}\right] \end{aligned} \tag{2.19}$$

where $\|\cdot\|$ denotes Frobenius matrix norm.

The intuition from Theorem 1 is that $\frac{1}{N}\mathbb{E}\left[\mathbf{F}_{\hat{\phi}}\right]$ can be well-approximated with $\frac{1}{N}\mathrm{F}_{\hat{\phi}}$ when value of N is large enough. For deviation probability to be less than predefined threshold $\eta \in (0, 1)$, the right-hand-side of (2.19) is bounded by η. Therefore, the number of CRs required is:

$$N \geq \frac{2\epsilon^2\gamma^4}{\sigma_s^4\delta_0^2\eta}\left[\frac{1}{2R^2R_0^2} - \frac{\log^2\left(R/R_0\right)}{\left(R^2 - R_0^2\right)^2}\right] \tag{2.20}$$

Using this approximation, the RMSE of RSS-only algorithm having uniform random CR placement is provided by:

$$\text{RMSE}_{R,U} \geq \left(\frac{2}{N f_{\hat{\phi}}\left(R, \gamma, \sigma_s^2\right)} \right)^{1/2} \tag{2.21}$$

where subscript R, U denotes RSS-only CRB for uniform CR placement.

2.3.2 Joint CRB For Uniform Random CR Deployment

A similar procedure as used for asymptotic RSS-only CRB is applied to derive asymptotic joint CRB from $\mathbf{F} = \mathbf{F}_{\widehat{\phi}} + \mathbf{F}_{\widehat{\boldsymbol{\theta}}|\widehat{\phi}}$. $\mathbf{F}_{\widehat{\boldsymbol{\theta}}|\widehat{\boldsymbol{\phi}}}$ is first rewritten from (2.13) as:

$$\begin{aligned} \frac{1}{N}\mathbf{F}_{\widehat{\boldsymbol{\theta}}|\widehat{\phi}} =& \frac{1}{N}\sum_{n=1}^{N}\left\{\left[\alpha d_n^{-(\gamma+2)}\cos^2\widetilde{\theta}_n + 2d_n^{-2}\tan^2\widetilde{\theta}_n\right]\right. \\ & \left.\times\begin{bmatrix}\sin\theta_n \\ -\cos\theta_n\end{bmatrix}[\sin\theta_n, -\cos\theta_n]\right\} \end{aligned} \tag{2.22}$$

From (2.22), it is observed that $\frac{1}{N}\mathbf{F}_{\widehat{\boldsymbol{\theta}}|\widehat{\boldsymbol{\phi}}}$ can be interpreted as ensemble average of a function of random variables θ_n and d_n, with statistical mean provided by:

$$\begin{aligned} \frac{1}{N}\mathbb{E}\left[\mathbf{F}_{\widehat{\boldsymbol{\theta}}|\widehat{\phi}}\right] =& \frac{1}{(R^2 - R_0^2)}\left[2\log\left(R/R_0\right)\left(\frac{\tan\theta_T}{\theta_T} - 1\right)\right. \\ & \left. - \frac{\alpha}{2\gamma}\left(R^{-\gamma} - R_0^{-\gamma}\right)\left(\frac{\sin 2\theta_T}{2\theta_T} + 1\right)\right]\mathbf{I}_2 \\ =& f_{\widehat{\boldsymbol{\theta}}|\widehat{\phi}}\left(R, \gamma, \sigma_s^2, \theta_T, \beta\right)\mathbf{I}_2 \end{aligned} \tag{2.23}$$

The deviation probability of ensemble average $\frac{1}{N}\mathbf{F}_{\widehat{\boldsymbol{\theta}}|\widehat{\boldsymbol{\phi}}}$ from statistical mean $\frac{1}{N}\mathbb{E}[\mathbf{F}] = \frac{1}{N}\mathbb{E}\left[\mathbf{F}_{\widehat{\phi}}\right] + \frac{1}{N}\mathbb{E}\left[\mathbf{F}_{\widehat{\boldsymbol{\theta}}|\widehat{\phi}}\right]$ is provided by the following theorem.

Theorem 2: (Deviation Probability of Joint FIM): For $\delta_0 > 0$, the deviation probability of joint FIM, which is provided by (2.24), is given below, where $f_n \triangleq \alpha d_n^{-(\gamma+2)}\cos^2\tilde{\theta}_n + 2d_n^{-2}\tan^2\tilde{\theta}_n$.

$$\Pr\left\{\left\|\frac{1}{N}\mathbf{F} - \frac{1}{N}\mathbb{E}[\mathbf{F}]\right\|_F > \delta_0\right\} < \frac{1}{N\delta_0^2}\left\{\frac{\epsilon^2\gamma^4}{\sigma_s^4 R^2 R_0^2} + \mathbb{E}\left[f_n^2\right] - \frac{1}{2}\left[\mathbb{E}\left[f_n\right] + \frac{2\epsilon\gamma^2\log\left(R/R_0\right)}{\sigma_s^2\left(R^2 - R_0^2\right)}\right]^2\right\} \tag{2.24}$$

$$N \geq \frac{1}{\eta\delta_0^2}\left\{\frac{\epsilon^2\gamma^4}{\sigma_s^4 R^2 R_0^2} + \mathbb{E}\left[f_n^2\right] - \frac{1}{2}\left[\mathbb{E}\left[f_n\right] + \frac{2\epsilon\gamma^2\log\left(R/R_0\right)}{\sigma_s^2\left(R^2 - R_0^2\right)}\right]^2\right\} \tag{2.25}$$

The intuition from Theorem 2 is that $\frac{1}{N}\mathbf{F}$ can be well-approximated with with $\frac{1}{N}\mathbb{E}[\mathbf{F}]$ when value of N is large enough. For deviation probability to be less than η, it is required to bound right-hand-side of (2.24) by η. The number of required CRs is then bounded by

(2.25). Using this approximation, the joint FIM and corresponding RMSE are provided by:

$$\mathbf{F}_{J,U,C} = N\left[f_{\hat{\phi}}\left(R,\gamma,\sigma_s^2\right) + f_{\hat{\boldsymbol{\theta}}|\phi}\left(R,\gamma,\sigma_s^2,\theta_T,\beta\right)\right]\mathbf{I}_2 \tag{2.26}$$

$$\text{RMSE}_{J,U,C} \geq \left\{\frac{2}{N\left[f_{\widehat{\phi}}\left(R,\gamma,\sigma_s^2\right) + f_{\widehat{\boldsymbol{\theta}}|\widehat{\phi}}\left(R,\gamma,\sigma_s^2,\theta_T,\beta\right)\right]}\right\}^{1/2} \tag{2.27}$$

where subscript J,U,C denotes joint CRB for uniform CR placement using CRB evaluated using DoA estimation error variance.

Chapter 3

Practical Localization Algorithms

In this dissertation work, two cooperative localization algorithms are selected to study the achievable localization performance with respect to CRB derived in earlier chapters, one dealing with RSS-only localization and other one dealing joint RSS/DoA localization.

3.1 Weighted Centroid Localization

Considering the RSS-only case, WCL is range-free algorithm which provides location estimate and has low-complexity. In this algorithm, PU location is estimated as weighted average of all CR locations within the range of its transmission, where weights are dependent on RSS of each CR user. The WCL location estimate is provided by:

$$\widehat{\ell}_{P,WCL} = \sum_{n=1}^{N} \widehat{\psi}_n \ell_n / \sum_{n=1}^{N} \widehat{\psi}_n \tag{3.1}$$

WCL implemented using other weighting scheme also exists. Information about PU transmit power and channel condition is not required by WCL, and it is robust to shadowing variance as compared to range-based algorithms.

3.2 Weighted Stansfield Algorithm

For joint RSS and DoA case, we consider weighted Stansfield algorithm which is seen to perform better compared to other DoA fusion algorithms, like maximum likelihood algorithm solved by iterative methods. Estimated error variances, which are dependent on RSS, are weights for each DoA. The weighted Stansfield location estimates is provided

by $\widehat{\ell}_{P,St} = \left(\mathbf{A}_{St}^T \mathbf{W}^{-1} \mathbf{A}_{St}\right)^{-1} \mathbf{A}_{St}^T \mathbf{W}^{-1} \mathbf{b}_{St}$, where

$$\mathbf{A}_{St} = \begin{bmatrix} \sin\left(\widehat{\theta}_1\right) & -\cos\left(\widehat{\theta}_1\right) \\ \vdots & \vdots \\ \sin\left(\widehat{\theta}_N\right) & -\cos\left(\widehat{\theta}_N\right) \end{bmatrix},$$

$$\mathbf{b}_{St} = \begin{bmatrix} x_1 \sin\left(\widehat{\theta}_1\right) - y_1 \cos\left(\widehat{\theta}_1\right) \\ \vdots \\ x_N \sin\left(\widehat{\theta}_N\right) - y_N \cos\left(\widehat{\theta}_N\right) \end{bmatrix} \tag{3.2}$$

and weighting matrix is expressed as $\mathbf{W} = \text{diag}\left[\widehat{\sigma}_1^2, \ldots, \widehat{\sigma}_N^2\right]$, where $\widehat{\sigma}_n^2$ is achieved by replacement of true DoA θ_n with estimated DoA $\widehat{\theta}_n$ in (2.3) or (2.4).

Chapter 4

Simulation Results

4.1 Simulation Settings

The basic parameter settings used in the simulations are summarized in this section. The CRs are placed in circle having radius $R = 150$m and guard region $R_0 = 5$m which is centered around PU with location $\ell_P = [0, 0]^T$ and for simplicity. The power transmitted by PU P_T is set as 20dBm (100mW). The power of measurement noise P_M is set as 80dBm (10pW) which provides moderate estimate of noise. The path-loss exponent is $\gamma = 5$ and shadowing standard deviation is $\sigma_s = 6$dB . Every CR is equipped with ULA having $N_a = 2$ antennas and $N_s = 50$ samples are used for each localization period. It is assumed that array orientation error with respect to incoming DoA follows uniform distribution provided by $\widetilde{\theta}_n \sim \mathcal{U}(-\pi/3, \pi/3)$. Parameter $\pi/3$ is used for array orientation error as maximum orientation error, which is $\pi/2$, leads to infinite error variance which can can be validated through (2.3) or (2.4), therefore $\pi/3$ is a practical value. Each data point in the results is achieved by averaging for 1000 CR placements and 2000 realization of RSS/DoA measurement if applicable. In the following simulation results, these settings are used unless stated otherwise.

4.2 Simulation Results

Impact of node density on localization accuracy is studied. The results for WCL algorithm and RSS-only CRB are presented in Fig. 4.1. Steady performance improvement can be observed for RSS-only CRB and WCL algorithm on addition of more CRs, and WCL algorithm maintains RMSE gap of around 10m for considerably large number of

CRs, say 40, in comparison to RSS-only CRB.

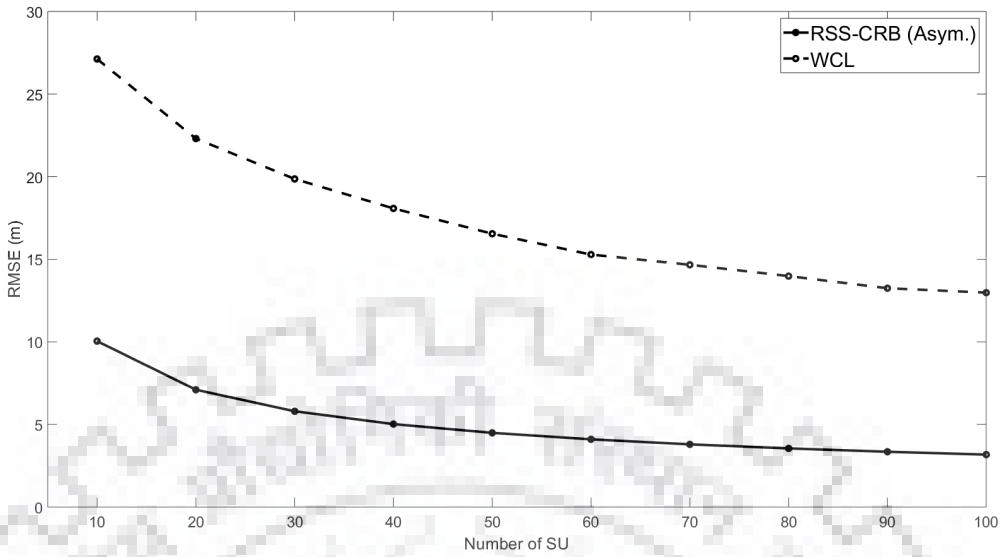

Fig. 4.1. Comparison of RMSE for RSS-only CRB and WCL having varying number of CRs in uncorrelated shadowing environment(σ_s=6dB), with uniform random deployment in circle with R = 150m.

The gap is due to the fact that WCL does not make any assumption about the information of channel condition, such as shadowing variance, while evaluation of CRB makes use of such information. The derived joint CRB output evaluated using optimal DoA estimators, Stansfield algorithm and weighted Stansfield algorithm are shown in Fig. 4.2. The accuracy of joint CRB and weighted Stansfield algorithm varies from 0.1 meters to 1.5 meters, in comparison to accuracy range of 5 to 25 meters for WCL and RSS-only CRB in Fig. 4.1, and 1 to 2.5 meters for Stansfield algorithm, clearly indicating that by using RSS and DoA measurement leads to more accurate location estimate compared to using only RSS or DoA.

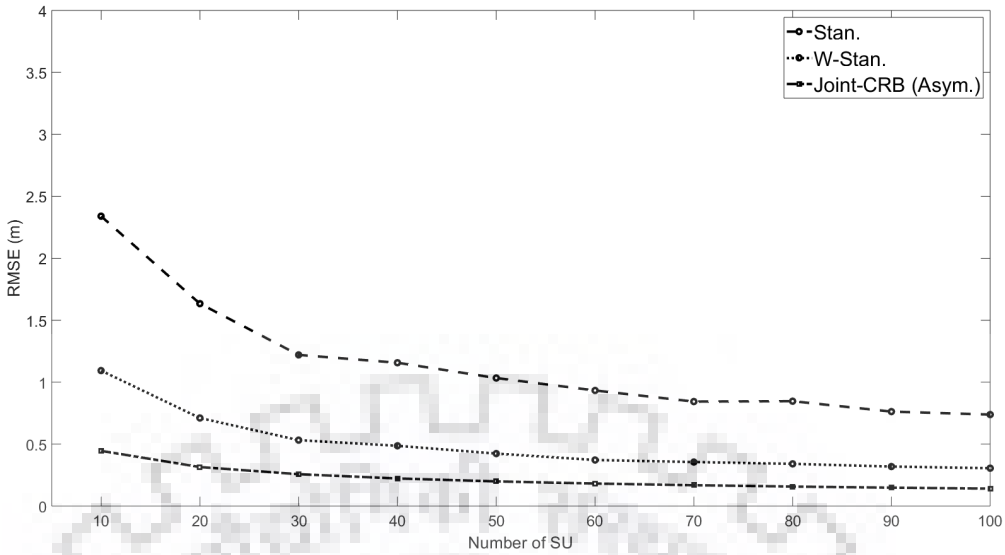

Fig. 4.2. Comparison of RMSE for joint CRB, Stansfield algorithm and weighted Stansfield algorithm having varying number of CRs in uncorrelated shadowing environment (σ_s=6dB), with uniform random deployment in circle with R = 150m.

Accuracy of asymptotic CRBs derived in chapter 2 for uniform random CR deployment is evaluated and compared with the exact CRBs derived in chapter 4 conditioned on specific CR placement. From (2.20) and (2.25) it can be observed that number of CRs required to make asymptotic CRB accurate is dependent on number of nodes. It was that observed the value of R_0/R plays key role in determination of required N. Thus comparison of exact CRBs, obtained after numerically averaging over uniform random CR placements, with asymptotic CRBs for R_0/R=0.33, where results are shown in Fig. 4.3 and Fig. 4.4 for RSS-only bounds and joint bounds. For RSS-only bounds, asymptotic CRB approaches exact bounds, in that difference is less than 2.5 meters for N=40. It should be noted that RMSE increases as R_0 is increased since CRs that are closer to PU are excluded. It can be observed from Fig. 4.4 that the approximation improves drastically for $N > 40$ when R_0/R=0.33.

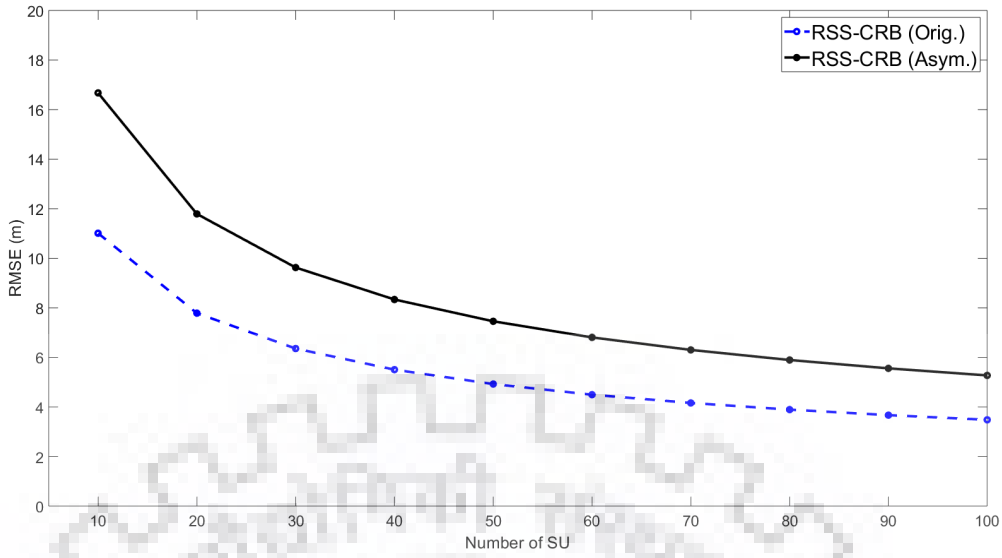

Fig. 4.3. Comparison of exact and asymptotic RMSE for RSS-only CRB having varying number of CRs in uncorrelated shadowing environment(σ_s =6dB), for R_0/R=0.33.

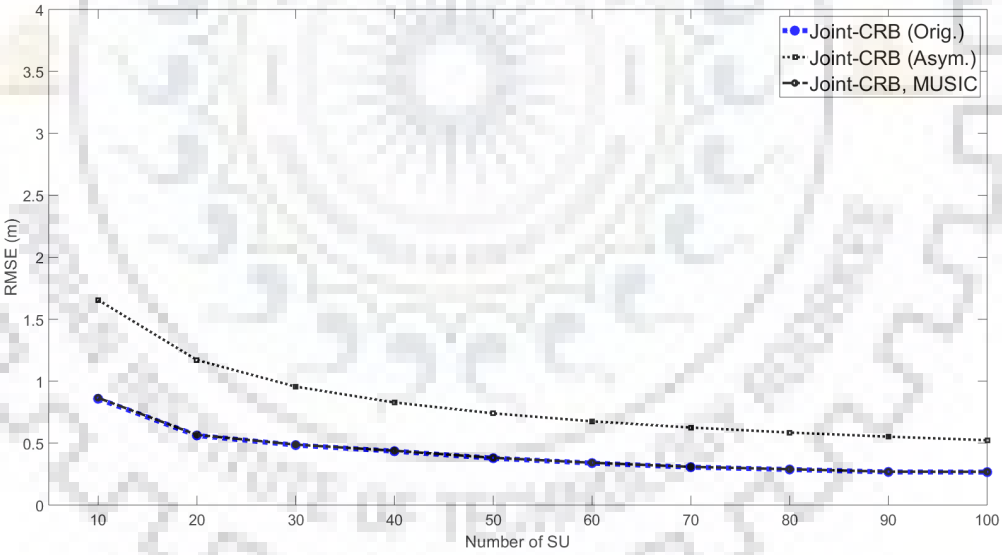

Fig. 4.4. Comparison of exact and asymptotic RMSE for joint CRB having varying number of CRs in uncorrelated shadowing environment(σ_s =6dB), for R_0/R=0.33.

In Fig. 4.5, a comparative view of outputs for RMSE of RSS-only CRB and Joint-CRB is provided clearly depicting that as DoA estimation accuracy is significantly dependent on RSS, and practical algorithms show that using both RSS and DoA estimates helps in providing improved localization accuracy compared to DoA alone, therefore CRB for

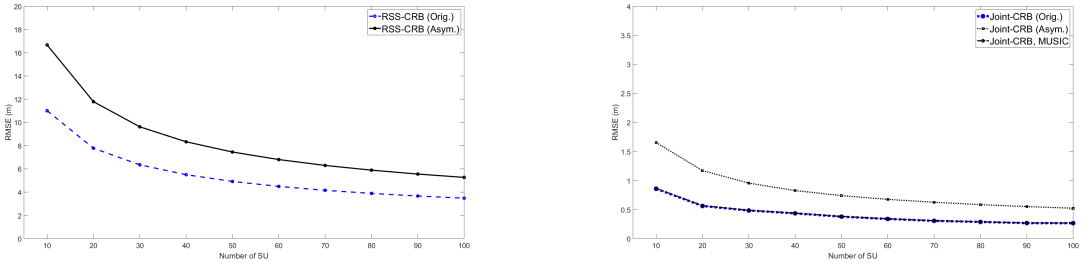

Fig. 4.5. Comparative view of RMSE RSS-only CRB and Joint-CRB CRB having varying number of CRs in uncorrelated shadowing environment(σ_s =6dB), for R_0/R=0.33.

joint RSS and DoA-localization is far more efficient in characterizing localizing ability of CR network.

Chapter 5

SR-based PU Localization

The problem of localizing source making use of range and range-difference measurements accumulated using network of passive receiver has observed significant attention in literature due to their significance in many areas including teleconferencing, navigation, and geophysics.

In [6], localization using range and range-difference are discussed. Therefore, in this work, robust statistics methods are applied on squared range measurements and two different methods are implemented to solve the issue of PU localization when some CRs are outlying. The first approach is efficient in terms of computational complexity, but only objective convergence is guaranteed theoretically in that approach. Contrary to that, whole-sequence converges in the second method. In order to take benefits of both the approaches, a hybrid algorithm is developed by integrating both the approaches that offers computational efficiency along with whole-sequence convergence.

5.1 System Model

In the model used for robust PU localization in presence of outliers, the system comprises of R CRs, with locations which is known, and location of PU is estimated by usage of range measurement observed by CRs. The measurements are collected by a central processing node and then the location of PU is computed. Each CR report range estimates, expressed as r_i, given by:

$$r_i = \|x - a_i\|_2 + v_i, \quad i = 1, \ldots, R \tag{5.1}$$

where $\|\cdot\|_2$ represents Euclidean distance, $\boldsymbol{x} \in \mathbb{R}^n$ is coordinate of PU, $a_i \in \mathbb{R}^n$ is location of i^{th} CR and v_i is modelling the measurement error. It is quite clear that n = 2 or 3 for

our required applications .

It is assumed that measurement errors v_i are independent and identically distributed random variable. For modelling the outlier measurements, measurement errors are assigned two-mode mixture PDF, which can be expressed as:

$$p_V(v) = (1-\beta)\mathcal{N}\left(v; 0, \sigma^2\right) + \beta\mathcal{H}(v) \tag{5.2}$$

Therefore, measurement errors are drawn with probability $1-\beta$ from distribution $\mathcal{N}\left(v; 0, \sigma^2\right)$ or with probability β from distribution $\mathcal{H}(v)$. $\mathcal{N}\left(v; 0, \sigma^2\right)$ is used for modelling the measurement noise for measurements which are outlier-free, which is Gaussian distribution with zero mean and variance σ^2, and $\mathcal{H}(v)$ is used to model the outlier errors. Hence, probability β, also known as contamination ratio, represents ratio of outlier measurement to all the measurement. The outlier error distribution, $\mathcal{H}(v)$, is generally modeled with shifted Gaussian distribution [15], Uniform distribution [16], an exponential distribution [17] or a Rayleigh distribution [18].

Here, the primary goal is estimation of x by usage of measurements r_i, $i = 1, \ldots R$, while measurements from outlier CRs are disregarded. The fusion node has no knowledge regarding number of outlier CRs and outlier measurements distribution. Moreover, a assumption is made that all the measurements which are reported including noisy and irrelevant measurements are non-negative. For that purpose, robust statistics is exploited and methods are proposed to obtain the solution.

Chapter 6

Squared Range Based Robust Localization

In this module, robust statistics is applied to squared range measurements to develop a localization method. Though this method is not optimum in the ML sense, the solution to the problem can be obtained. The square-range-based least squares (SRLS) objective can be formulated as follows [6]:

$$\underset{\boldsymbol{x}}{\text{minimize}} \sum_{i=1}^{R} \left(\|\boldsymbol{x} - \boldsymbol{a_i}\|_2^2 - r_i^2 \right)^2 \tag{6.1}$$

It is clearly evident that problem stated in (6.1) is non-convex. However, (6.1) can be transformed into special category of optimization problem by rephrasing it as minimization problem with a constraint provided by [6, 14] :

$$\begin{aligned} \underset{\boldsymbol{x},\boldsymbol{\alpha}}{\text{minimize}} \quad & \textstyle\sum_{i=1}^{R} \left(\alpha - 2a_i^T \boldsymbol{x} + \|a_i\|^2 - r_i^2 \right)^2 \\ \text{subject to} \quad & \|\boldsymbol{x}\|^2 = \alpha \end{aligned} \tag{6.2}$$

It is noteworthy that α is not parameter to be set but a resultant of optimization procedure. The measurements from outlier CRs which are not reliable affect localization accuracy significantly in this formulation. Robust statistics is used for decreasing the sensitivity of estimator for common assumption. The robustness here expresses insensitive behaviour of the estimator to minor deviations from common assumptions, which is Gaussian distributed noise. In (6.2), β expresses deviation from this assumption. The primary objective is dealing with unknown distribution $\mathcal{H}(v)$ and to attain distributional robustness.

The statistical procedure must be having following attributes, as described in [19]. It should be efficient, i.e. it must be having near optimum performance at presumed model,

i.e., noise having Gaussian distribution. It should be stable, i.e., it must be insensitive to minor deviations from presumed model. Also, a catastrophe must not occur in case of large deviation from the model or breakdown. The general method to robustize statistical procedures is by decomposition of observed values into fitted values and the residuals [19]. In the implemented methods, it is tried to figure out residuals and re-fit them in a iterative manner until objective function converges. Each term of (6.2) reflects residual obtained from single CR. These residuals can be used for re-fitting observations in a iterative manner.

Specifically, residuals are used to assign weight to each observation. A larger weight should be assigned to an observation if it is fitted to the model and therefore it should have greater role in making a decision. Taking inspiration from [20], the objective function is defined as:

$$\mathcal{J}(\boldsymbol{y}, \boldsymbol{w}) = \sum_{i=1}^{R} w_i \left(\tilde{a}_i^T y - b_i\right)^2 + \sum_{i=1}^{R} \epsilon^2 w_i - \ln w_i \tag{6.3}$$

where $y = \begin{bmatrix} x & \alpha \end{bmatrix}^T$, $\tilde{a}_i^T = \begin{bmatrix} -2a_i^T & 1 \end{bmatrix}$, $b_i = r_i^2 - \|a_i\|^2$, and $w \in \mathbb{R}^R$ is weight vector with $w_i > 0, \forall i$. The ϵ parameter is function of standard deviation of noise which is set as $\epsilon = 1.34\sqrt{3}\sigma$.

The first summation given in the objective function (6.3) represents the weighted version of objective in (6.2). The other terms in (6.3) are added in such a way that leads to development Geman-McClure (GM) function [21]. The goal of GM function is reduction of the effect of large errors, by interpolation between ℓ_0 and ℓ_2 norm minimization [21].

The primary aim is minimization of $\mathcal{J}(\boldsymbol{y}, \boldsymbol{w})$ over y and w. Specifically, the following optimization problem is being solved:

$$\begin{aligned} \underset{\boldsymbol{y},\boldsymbol{w}}{\text{minimize}} \quad & \mathcal{J}(\boldsymbol{y}, \boldsymbol{w}) \\ \text{subject to} \quad & \boldsymbol{y}^T \boldsymbol{D} \boldsymbol{y} + 2\boldsymbol{f}^T \boldsymbol{y} = 0 \\ & w_i > 0, \forall i \end{aligned} \tag{6.4}$$

where

$$D = \begin{bmatrix} I_n & 0_{n\times 1} \\ 0_{1\times n} & 0 \end{bmatrix}, f = \begin{bmatrix} 0_{n\times 1} \\ -0.5 \end{bmatrix} \tag{6.5}$$

The implemented algorithms exploits an alternative approach to update y and w. The initialization is started by taking $w_i^{(0)} = 1, \forall i$ .Then at k^{th} iteration, for updating y, the following optimization problem is solved :

$$y^{(k+1)} = \arg\min \quad \mathcal{J}\left(y, w^{(k)}\right)$$

$$\text{subject to} \quad y^T D y + 2 f^T y = 0 \tag{6.6}$$

In a similar manner, the updation of weights takes place as follows:

$$\begin{aligned} \boldsymbol{w}^{(k+1)} &= \arg\min \quad \mathcal{J}\left(y^{(k+1)}, \boldsymbol{w}\right) \\ &\text{subject to} \quad w_i > 0, \forall i \end{aligned} \tag{6.7}$$

The above defined optimization is convex in nature and therefore, a global solution could be achieved comfortably. Therefore, weights are provided by:

$$w_i^{(k)} = \frac{1}{\left(e_i^{(k)}\right)^2 + \epsilon^2} \tag{6.8}$$

where $e_i^{(k)} = \tilde{\boldsymbol{a}}_{\boldsymbol{i}}^T \boldsymbol{y}^{(k)} - b_i$.

It is common to choose such weights in IRLS methods [19, 21]. In robust statistics, the observed values are bifurcated into fitted values $y^{(k)}$ and residuals $e^{(k)}$ after every iteration. Residuals are then used for tuning and updating the observations weights. In case the residuals are large, i.e., $e_i \gg \epsilon$, each term of first summation in (6.3), is tending to 1. In a similar manner, when residuals are small, each term tends to zero in the summation. It can be inferred that large residuals observations are being minimized.

Then, two different methods are being introduced for finding solution of (6.6). In the first method, it can be seen that (6.6) is mapped to Generalized Trust Region Subproblems (GTRS) [14]. Then, the exact solution at every iteration is obtained by employing GTRS formulation. In the second method, a gradient descent based approach is introduced for solving the required optimization problem. Although this method is computationally inefficient when compared to first method, it provides a number of desirable attributes.

6.1 Squared Range Iterative Reweighted Least Squares (SR-IRLS) Method

The problem in (6.6) is reformulated in matrix form as:

$$\begin{aligned} \underset{\boldsymbol{y}}{\text{minimize}} \quad & (\boldsymbol{A}\boldsymbol{y} - \boldsymbol{b})^T \boldsymbol{W}^{(k-1)} (\boldsymbol{A}\boldsymbol{y} - \boldsymbol{b}) \\ \text{subject to} \quad & \boldsymbol{y}^T \boldsymbol{D} \boldsymbol{y} + 2\boldsymbol{f}^T \boldsymbol{y} = 0 \end{aligned} \tag{6.9}$$

where

$$A = \begin{bmatrix} -2a_1^T & 1 \\ \vdots & \vdots \\ -2a_R^T & 1 \end{bmatrix}, b = \begin{bmatrix} r_1^2 - \|a_1\|^2 \\ \vdots \\ r_R^2 - \|a_R\|^2 \end{bmatrix}, \tag{6.10}$$

and $W^{(k)}$ is a diagonal weighting matrix for k^{th} iteration and $w_i^{(k)}$ is i^{th} diagonal entry of $W^{(k)}$, $i = 1, \dots R$. It should be noted that in (6.9), minimization of quadratic objective function is taking place on being subjected to quadratic equality constraint. Therefore, this special category of optimization problems are referred as Generalized Trust Region Subproblem (GTRS) [14]. This optimization problem is non-convex due to the equality constraint. However, it can be seen that global solution of GTRS problems can be achieved efficiently [6, 14].

SRILS algorithm, given below, depicts the procedure to calculate the estimate of (6.9) using the theorems from [14].

SRILS Algorithm

Require: a_i, r_i for $i = 1, \dots, R, \epsilon$, maximum number of iterations *maxIter*, and the convergence tolerance Δ

1. **Compute** A, b, D, and f using (6.5) and (6.10)
2. **Initialize** $w_i^{(0)} = 1, \forall i$, and $k = 1$
3. **Repeat**:
4. $\lambda_l = \max\left\{-\left(\boldsymbol{A}^T\boldsymbol{W}^{(k-1)}\boldsymbol{A}\right)_{ii}, i = 1, \dots, n\right\}$
5. **Find** λ^* : solve $\boldsymbol{y}(\lambda)^T\boldsymbol{D}\boldsymbol{y}(\lambda) + 2\boldsymbol{f}^T\boldsymbol{y}(\lambda) = 0$ using a bisection algorithm in interval (λ_l, ∞) , where $\boldsymbol{y}(\lambda) = \left(\boldsymbol{A}^T\boldsymbol{W}^{(k-1)}\boldsymbol{A} + \boldsymbol{\lambda}\boldsymbol{D}\right)^{-1}\left(\boldsymbol{A}^T\boldsymbol{W}^{(k-1)}\boldsymbol{b} - \lambda\boldsymbol{f}\right)$
6. **Update** $y : y^{(k)} = y\left(\lambda^*\right)$
7. **Update** $w^{(k)}$ using (6.8)
8. **Until** Convergence, i.e., if $\left|\mathcal{J}\left(y^{(k)}, w^{(k)}\right) - \mathcal{J}\left(y^{(k-1)}, w^{(k-1)}\right)\right| < \Delta$ or the maximum number of iterations *maxIter* is reached.

On inspecting above algorithm, it is observed that matrix inversions are required for $(n + 1) \times (n + 1)$ matrices only, where n represents space dimension and is equivalent to 2 . Therefore, the primary computational complexity of algorithm arises from matrix multiplications. Therefore, the primary computational complexity of SR-IRLS algorithm is due to number of iterations.

Simulations prove that SR-IRLS method requires less time for solving the optimization procedure. However, due to non-convexity, it is not guaranteed that whole-sequence of the iterates converges .

This leads to look for a globally convergent algorithm. In next section, an new method is discussed for solving (6.9) based on gradient descent. Then both the methods are integrated to get to globally convergent and computationally efficient method.

6.2 Squared Range Gradient Descent (SR-GD) Method

In this section, SR-GD algorithm is discussed in order to solve optimization problem in (6.6) which is based on gradient descent and for which whole-sequence of iterates converges and it is proven theoretically in [22]. For solving that purpose, Lipschitz continuity of objective function gradient along with objective having a special form and constraint are used. Simulations show that this method requires more number of iterations for converging compared to SR-IRLS. The primary objective is to use both the methods in order to implement a hybrid method. Taking inspiration from [22], $y^{(k)}$ is updated at each iteration as follows:

$$\begin{aligned} y^{(k)} = \arg\min_{y} & \left\langle \nabla_y \mathcal{J}\left(\hat{y}^{(k)}, w^{(k-1)}\right), y - \hat{y}^{(k)} \right\rangle \\ & + l^{(k)} \left\| y - \hat{y}^{(k)} \right\|_2^2 \\ \text{subject to} \quad & y^T D y + 2 f^T y = 0, \end{aligned} \tag{6.11}$$

where

$$\hat{y}^{(k)} = y^{(k-1)} + \omega^{(k)} \left(y^{(k-1)} - y^{(k-2)} \right) \tag{6.12}$$

and $l^{(k)}$ is Lipschitz constant of $\nabla_{\boldsymbol{y}} \mathcal{J}\left(\boldsymbol{y}, \boldsymbol{w}^{(k-1)}\right)$ at k^{th} iteration. Lipschitz continuity is defined as:

$$\left\| \nabla_{\boldsymbol{y}} \mathcal{J}\left(\boldsymbol{u}, \boldsymbol{w}^{(k-1)}\right) - \nabla_{\boldsymbol{y}} \mathcal{J}\left(\boldsymbol{v}, \boldsymbol{w}^{(k-1)}\right) \right\| \leq l^{(k)} \|\boldsymbol{u} - \boldsymbol{v}\| \tag{6.13}$$

It can be inferred using intuition that first term of the objective figures out the steepest descent, while second term prevents substantial changes in the magnitude of gradient. The Lipschitz constant of gradient function limits size of step the algorithm and new estimate $y^{(k)}$ is forced to be around prediction $\hat{y}^{(k)}$. The new prediction is calculated using the extrapolation factor $\omega(k) = \frac{1}{12}\sqrt{\frac{l^{(k-1)}}{l^{(k)}}}$ and previous iterates [22]. w is updated in similar manner as (6.8).

This problem is also non-convex, but whole-sequence convergence of the algorithm is proved in [22] by exploitation of the characteristics of objective. It is easily noticeable

that optimization problem formulated in (6.11) is a GTRS problem. This is due to minimization of quadratic objective subjected to a quadratic equality constraint. SR-GD algorithm shows the steps to find the solution of the localization problem.

SR-GD Algorithm

Require: a_i, r_i for $i = 1, \ldots, R, \epsilon$, maximum number of iterations *maxIter*, and convergence tolerance Δ .

1. **Compute** A, b, D, and f using (9.5) and (9.10)
2. **Initialize** $W^{(0)}$ with identity matrix, $y^{(-1)} = y^{(0)} = A^{\dagger}b, l^{(0)} = 0$, and $k = 1$
3. **Repeat**:
4. $l^{(k)} = 2 \left\| \boldsymbol{A}^T \boldsymbol{W}^{(k-1)} \boldsymbol{A} \right\|_F$
5. $\omega^{(k)} = \frac{1}{12} \sqrt{\frac{l^{(k-1)}}{l^{(k)}}}$
6. $\hat{\boldsymbol{y}}^{(k)} = \boldsymbol{y}^{(k-1)} + \omega^{(k)} \left(\boldsymbol{y}^{(k-1)} - \boldsymbol{y}^{(k-2)} \right)$
7. **Find** λ^* : solve $y(\lambda)^T D y(\lambda) + 2 f^T y(\lambda) = 0$ using bisection algorithm in interval $\left(-l^{(k)}, \infty\right)$, where $y(\lambda) = \left(l^{(k)} I_{n+1} + \lambda D\right)^{-1} \left(-A^T W^{(k-1)} \left(A \hat{y}^{(k)} - b\right) + l^{(k)} \hat{y}^{(k)} - \lambda f\right)$
8. **Update** $y : y^{(k)} = y\left(\lambda^*\right)$
9. **Update** $w^{(k)}$ using (9.8)
10. **Until** Convergence, i.e., if $\left\| y^{(k)} - y^{(k-1)} \right\| < \Delta$ or the maximum number of iterations *maxIter* is reached.

The simulations shows that SR-GD method requires more iterations to obtain the solution when compared to SR-IRLS. This is because in SR-GD, the value of new iterate is bounded around previous iterates, which is not the case in SR-IRLS algorithm.

6.3 Squared Range Hybrid (SR-Hybrid) Method

In order to reap the benefits of SR-IRLS method fast objective convergence as well as SR-GD whole sequence convergence, a hybrid approach is implemented in this work. To be

precise, SR-IRLS method is first implemented and iterates are updated by steps stated in SR-IRLS method. After the objective function converges, the steps mentioned in SR-GD method are implemented to get conclusive solution.

Chapter 7

Numerical Results

In this chapter, simulation results are presented to evaluate the performance of PU localization methods implemented in this work. Performance of the algorithms are compared with respect to various parameters such as RMSE, time etc. Robustness with respect to outlier measurement error distribution of the implemented algorithms is examined. A uniform distribution is obeyed by the outlier measurements, which models harsh environment.

The parameters used for simulation are set as follows. The CRs and PU are distributed uniformly at random in a $4000 \times 4000m^2$ area. The range measurements are distorted by AWGN having standard deviation of $\sigma = 55$m. The outlier CRs noises are distributed uniformly in range$[-4000\sqrt{2}, 4000\sqrt{2}]$. The distribution of measurement error is defined mathematically as follows:

$$p_V(v) = (1-\beta)\mathcal{N}\left(v; 0, \sigma^2\right) + \beta\mathcal{U}\left(v; -D_{\max}, D_{\max}\right), \tag{7.1}$$

where $\mathcal{U}\left(v; -D_{\max}, D_{\max}\right)$ is uniform distribution with support $[-D_{\max}, D_{\max}]$, which models outlier measurements. $\mathcal{N}\left(v; 0, \sigma^2\right)$ is zero mean Gaussian distribution having variance σ^2. The performances of implemented algorithms are compared with reference to RMSE,

$$\sqrt{\frac{1}{n}\|\boldsymbol{x} - \widehat{\boldsymbol{x}}\|_2^2} \tag{7.2}$$

averaged over sufficiently large number of random simulations. In this simulations, $\beta = 0.4$ i.e., 40% of the CRs are providing outlier measurements to fusion node.

From Fig. 7.1, it can be observed that the SR-based robust statistics methods perform better as compared to the practical localization algorithms i.e. WCL and W-Stansfield algorithm as well as from SR-LS algorithm in presence of outlying CRs. SR-hybrid

gives the best performance among all the algorithms and converges to CRLB requiring minimum number of secondary users (SU). Fig. 7.1 also shows that PU localization methods accuracy increases substantially as the number of SUs increases. Moreover, it can be clearly observed that the implemented methods tend to meet the CRB for large number of SU.

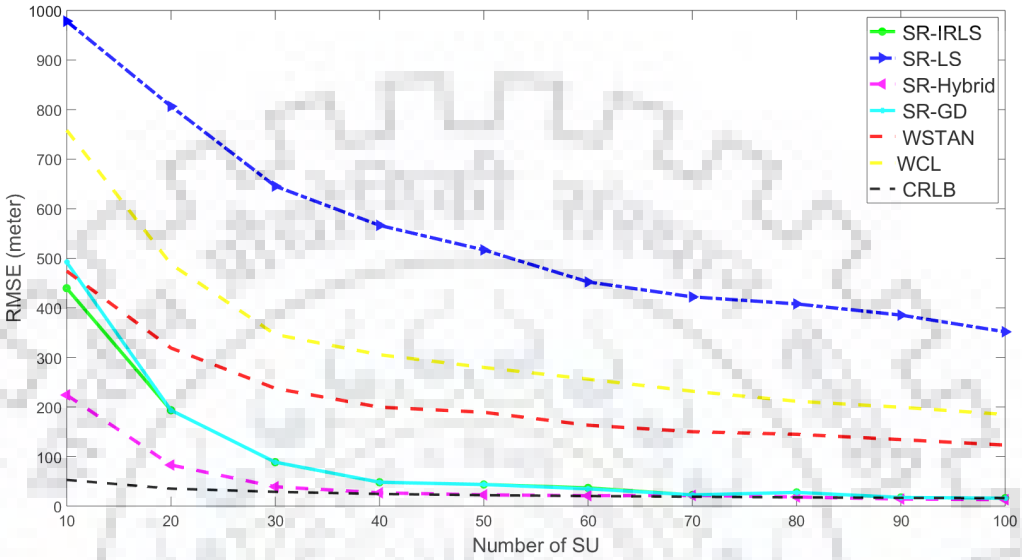

Fig. 7.1. RMSE of localization methods against number of SUs for $\beta = 0.4$ and 500 Monte Carlo trials.

From Fig. 7.1 and Fig. 7.2, it can be inferred that the implemented SR-based approaches perform efficiently for the given simulation settings, as they are unbiased and meet CRB .

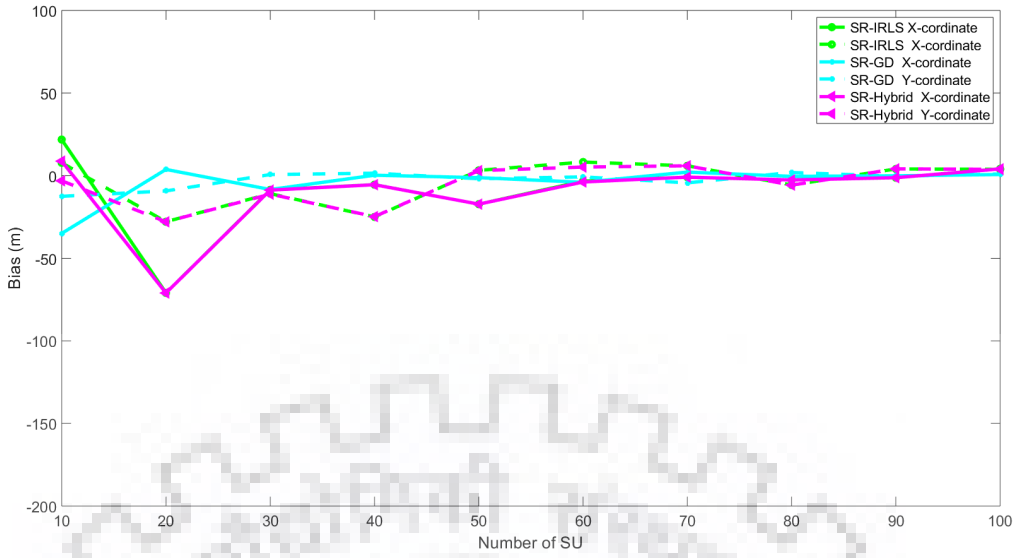

Fig. 7.2. Bias of localization methods against number of SUs for $\beta = 0.4$ and 500 Monte Carlo trials..

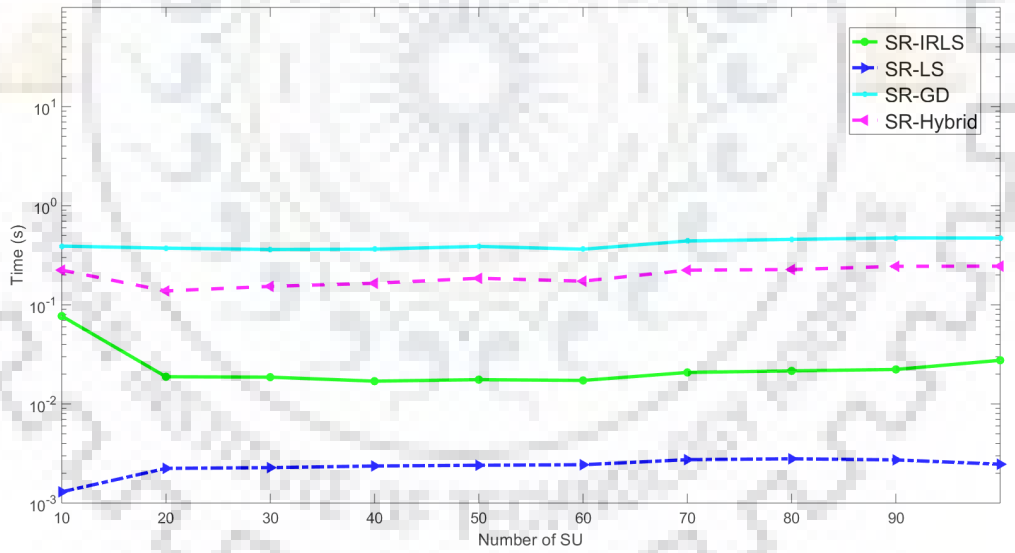

Fig. 7.3. Timing performance of localization methods against number of SUs for $\beta = 0.4$ and 500 Monte Carlo trials.

Fig. 7.3 presents the running times of SR-based localization algorithms for different number of SUs. It can be clearly observed that iterative methods needs more time for computation as compared to SR-LS. It is observable in Fig. 7.3 that the running time required by hybrid method is more when compared to SR-IRLS, but less when compared

to SR-GD .

It is noteworthy to analyze the performances of the localization methods when range measurements are distorted only by AWGN and no CR is reporting unreliable measurements, i.e. $\beta = 0$. It is observable in Fig. 7.4, the SR-LS method outperforms other methods in this case. There was such expectation from SR-LS method since LS methods are developed mainly to take care of Gaussian noise, while robust SR-based methods are developed to take care of outlier measurement. Therefore, there is trade-off between efficiency and stability as efficiency is sacrificed for $\beta = 0$, in order to attain stable performance when there is deviations from assumed model. But, it is easily noticeable that RMSE of robust SR-based algorithms is not much higher when compared to the RMSE for SR-LS method, which infers near optimum performance for AWGN.

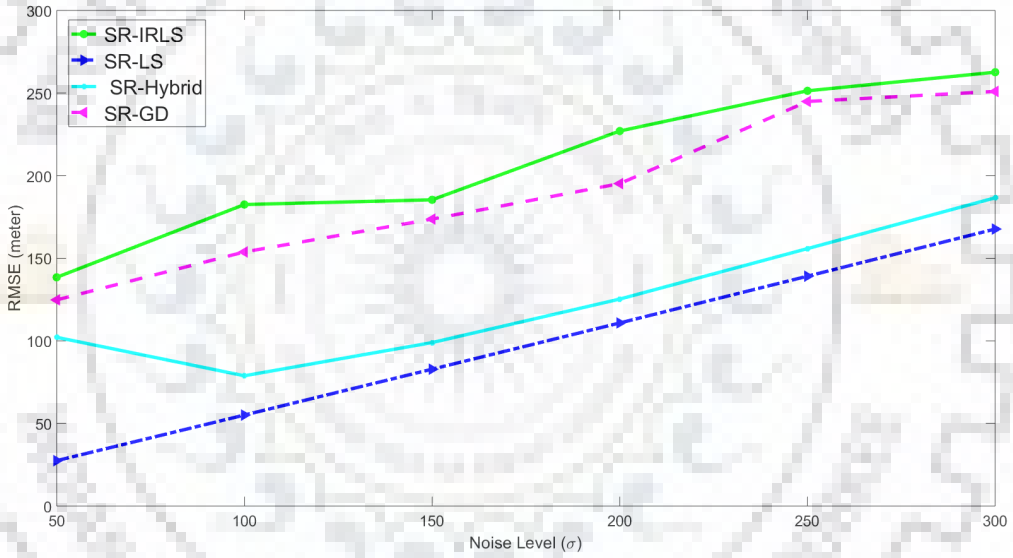

Fig. 7.4. RMSEs of different algorithms in environment with no outlier sensor i.e., β=0 for 500 Monte Carlo trials.

Chapter 8

Conclusion

In this dissertation, various algorithms for PU localization in CR networks are implemented and their performance is compared to each other with respect to RMSE, time and number of SUs. First a framework is presented to examine achievable performance of PU localization algorithms at the transmitter end in CR networks, which considers the DoA is dependent on RSS. Joint CRB for fixed CR deployment is derived, for both optimal DoA estimator and MUSIC algorithm. Following that joint CRB for uniform CR placement is derived. Then, using joint CRBs along with simulations results, the effect of number of CRs on joint CRB and practical localization algorithms (WCL and W-Stansfield) is examined and quantified.

Then the primary task is further extended by considering the problem of localizing single PU when contaminated measurements from different CRs with unknown probability distribution are present. For that purpose, the squared-range objective is formulated and exploited. In order to negate the effect of unreliable measurements and in order to find the location estimates using outlier-free measurements, robust statistics is being used. Then optimization procedure at hand is transformed into GTRS. Two methods(SR-IRLS and SR-GD) and a hybrid method are implemented to solve the problem. Simulations shows that the robust algorithm perform better compared to the practical localization methods and other methods implemented in this work, while providing satisfactory performance for Gaussian noise.

Bibliography

[1] J. Wang, J. Chen, and D. Cabric, "Cramer-Rao Bounds for Joint RSS / DoA-Based Cognitive Radio Networks," *IEEE Transactions on Wireless Communications*, vol. 12, no. 3, pp. 1363–1375, 2013.

[2] J. Mitola and G. Q. Maguire, "Cognitive Radio: Making Software Radios More Personal," *IEEE Personal Communications*, vol. 6, no. 4, pp. 13–18, 1999.

[3] S. Haykin, "Cognitive radio: brain-empowered wireless communications," *IEEE Transactions on Aerospace and Electronic Systems*, vol. 23, no. 2, pp. 201–220, 2005.

[4] H. Celebi and H. Arslan, "Utilization of location information in cognitive wireless networks," *IEEE Wireless Communications Magazine*, vol. 14, no. 4, pp. 6–13, 2007.

[5] N. Patwari, J. N. Ash, S. Kyperountas, A. O. Hero, R. L. Moses, and N. S. Correal, "Locating the nodes: cooperative localization in wireless sensor networks," *IEEE Signal Processing Magazine*, vol. 22, no. 4, pp. 54–69, 2005.

[6] P. S. Amir Beck, Jian Li, "Exact and Approximate Solutions of Source Localization Problems," *IEEE Transactions on Signal Processing*, vol. 56, no. 5, pp. 1770–1778, 2008.

[7] R. Stansfield, "Statistical theory of d.f. fixing," *JJ. Inst. Electr. Eng*, vol. 94, no. 15, pp. 762–770, 1947.

[8] A. W. M. Gavish, "Performance analysis of bearing-only target location algorithms," *IEEE Transactions on Aerospace and Electronic Systems*, vol. 28, no. 3, pp. 817–828, 1992.

[9] N. A. P. Stoica, "MUSIC, Maximum Likelihood, and Cramer-Rao Bound," *IEEE Transactions on Acoustics, Speech, and Signal Processing*, vol. 37, no. 5, pp. 720–741, 1989.

[10] Y. Jiang and M. R. Azimi-Sadjadi, "A Robust Source Localization Algorithm Applied to Acoustic Sensor Network," *Acoustics Speech and Signal Processing 2007. ICASSP 2007. IEEE International Conference*, vol. 3, no. 4, pp. 1233–1236, 2007.

[11] S. Yousefi, X. W. Chang, and B. Champagne, "Distributed cooperative localization in wireless sensor networks without NLOS identification," *2014 11th Workshop on Positioning, Navigation and Communication (WPNC)*, no. 3, pp. 1–6, 2014.

[12] M. G. A. Y. Zhang, K. Yang, "Robust target localization in moving radar platform through semidefinite relaxation," *2009 IEEE International Conference on Acoustics, Speech and Signal Processing*, no. 4, pp. 2209–2212, 2009.

[13] F. Gustafsson and F. Gunnarsson, "Mobile positioning using wireless networks: possibilities and fundamental limitations based on available wireless network measurements," *IEEE Signal Processing Magazine*, vol. 22, no. 4, pp. 41–53, 2005.

[14] J. J. More, "Generalizations Of The Trust Region Problem," *Optimization Methods and Software*, no. 2, pp. 189–209, 1993.

[15] F. G. A. M. Z. F. Yin, C. Fritsche, "TOA-Based Robust Wireless Geolocation and Cramér-Rao Lower Bound Analysis in Harsh LOS/NLOS Environments," *IEEE Transactions on Signal Processing*, vol. 61, no. 9, pp. 2243–2255, 2013.

[16] M. Hussain, Y. Aytar, N. Trigoni, and A. Markham, "Characterization of non-line-of-sight (NLOS) bias via analysis of clutter topology," *Record - IEEE PLANS, Position Location and Navigation Symposium*, no. 4, pp. 1247–1256, 2012.

[17] C. Pi-Chun, "A non-line-of-sight error mitigation algorithm in location estimation," *IEEE Wireless Communications and Networking Conference, WCNC.*, pp. 316–320, 1999.

[18] F. Yin and A. M. Zoubir, "Robust positioning in NLOS environments using nonparametric adaptive kernel density estimation," *ICASSP, IEEE International Conference on Acoustics, Speech and Signal Processing - Proceedings*, no. 3, pp. 3517–3520, 2012.

[19] G.-C. Rota, "Robust statistics," *Advances in Mathematics*, vol. 60, no. 1, pp. 123–205, 2004.

[20] I. Daubechies, R. Devore, M. Fornasier, and C. S. Güntürk, "Iteratively reweighted least squares minimization for sparse recovery," *Communications on Pure and Applied Mathematics*, vol. 63, no. 1, pp. 1–38, 2010.

[21] P. Pennacchi, "Robust estimate of excitations in mechanical systems using M-estimators-Theoretical background and numerical applications," *Journal of Sound and Vibration*, vol. 310, no. 45, pp. 923–946, 2008.

[22] Y. Xu and W. Yin, "A Globally Convergent Algorithm for Nonconvex Optimization Based on Block Coordinate Update," *Journal of Scientific Computing*, vol. 72, no. 2, pp. 700–734, 2017.